J Eng Math (2007) 57:303–315
DOI 10.1007/s10665-006-9089-3

ORIGINAL ARTICLE

Flow over compliant rotating disks

Peter W. Carpenter · Peter J. Thomas

Received: 12 June 2006 / Accepted: 10 August 2006 / Published online: 30 November 2006

Abstract Flow over compliant materials and compliant coatings has been studied for decades because of the potential of using such materials for laminar-flow control. Since boundary layers in most flows of engineering interest are three-dimensional the classic rotating-disk flow geometry, the paradigm for studying three-dimensional boundary layers, has been adapted to investigate flow over compliant rotating disks. This paper reviews the literature on the existing experimental and theoretical research on flow over compliant rotating disks. The article concludes by evaluating the status of the available results and their implications as regards future research routes to investigate the capabilities of compliant materials for laminar-flow control.

Keywords Compliant walls · Laminar-flow control · Rotating-disk flow

1 Introduction

The motivation for investigating the effects of wall compliance on laminar–turbulent transition in boundary layers dates back to suggestions by Gray [1] that dolphins achieve their high swimming speeds by controlling the boundary-layer flow over their compliant skin. The underlying idea is that the fluid flow over the dolphin's body is controlled by its interaction with the flexible, deformable dolphin skin in such a way that boundary-layer transition and turbulence are suppressed and, as a consequence, the skin-friction drag reduced. However, as pointed out by Carpenter et al. [2] most of the quantitative estimates contained in Gray's paper have in the meantime been shown to be inaccurate. Nevertheless, over the last twenty years it has also been clearly established, through experimental and theoretical investigations, that wall compliance can suppress the growth of Tollmien–Schlichting (TS) waves in boundary layers leading to substantial delays in the onset of laminar–turbulent transition (for reviews see [2–7]. Consequently compliant walls, or compliant coatings, are a viable method for drag reduction in such quasi-2D flow environments. But this favourable evidence really only applies to low-noise flow environments that are similar to the flat-plate boundary layer, for which amplification of TS waves is the primary route to transition. In many applications other, quite different, routes to transition may be dominant. This is likely to be the case, for example, for

P. W. Carpenter · P. J. Thomas (✉)
Fluid Dynamics Research Centre, School of Engineering, University of Warwick, Coventry CV4 7AL, UK
e-mail: pjt1@eng.warwick.ac.uk

three-dimensional (3D) boundary layers, particularly those developing over bodies with swept leading edges, flow past ships or, in fact, the flow over a dolphin's body.

In such 3D boundary layers inviscid instability mechanisms dominate that are much more powerful than TS waves. These are often associated with velocity profiles having inflexion points. An important example is, for instance, the cross-flow vortices that develop near the leading edge of a swept wing. These also develop in the 3D boundary layer over a rotating disk. This is one of the practical reasons why the rotating-disk flow has become the classic paradigm for studying flow instability and transition in fully 3D boundary-layer flow since the publication of the seminal paper by Gregory et al. [8].

Another attraction of the rotating disk is that it offers a relatively simple, perhaps deceptively simple, method for testing the drag-reducing capabilities of compliant coatings. All that is apparently required is a facility whereby a flat compliant disk rotates in a sufficiently large volume of water. In addition, accurate instrumentation is required for measuring the rotational speed and driving torque of the disk. Several investigations of this type have been carried out, some resulting in drag reduction. These are reviewed in Sect. 3.

The problem with just collecting data on torque as a function of rotational speed is that, because no information is available on the instabilities or turbulence characteristics, any change in effective drag cannot really be explained. For this reason the effects of wall compliance on flow stability and transition have recently been investigated fairly intensively through stability theory, numerical simulation, and experiment. The theoretical research will be reviewed in Sect. 4 and the experimental studies in Sect. 5. Very recently Cros et al. [9] have reported an experimental study of the effect of wall compliance on the flow structures previously observed by Schouveiler et al. [10] to develop in the narrow gap between rotating and stationary rigid disks. This work will be described in Sect. 6.

We presume that many readers will probably not be very familiar with the various mechanical properties and characteristics of compliant walls. With this in mind we will begin by providing a brief summary and overview of the quantities and the nomenclature required to follow our discussions.

2 Mechanical properties of compliant walls and nomenclature

Most experiments discussed in this paper relate to very simple flexible walls consisting of a single layer of viscoelastic material. A simple and common way to characterize viscoelastic material is by means of a complex elastic modulus $E^* = E' + \mathrm{j}E''$, where $\mathrm{j} = \sqrt{-1}$; E' is usually called the *storage* modulus and corresponds to the normal concept of elastic modulus used for Hookean solids. The non-dimensional factor E''/E' is usually termed the *loss factor* or *loss tangent*. The connection between E'' and the viscosity of the viscoelastic material can be readily seen for simple harmonic motion. An alternative to the modulus of elasticity for characterizing the viscoelastic materials is the modulus of rigidity $G^* = E^*/[2(1 + \nu_p)]$ where ν_p is the Poisson ratio. For the elastomeric materials used for compliant walls the material is virtually incompressible so that $\nu_p \simeq 0.5$ and $G^* \simeq E^*/3$. In general, both storage modulus, E', and loss factor, E''/E', and, consequently, G^* vary with the frequency of rotation of the disk (see Fig. 1). In both cases the SI unit is the Pascal or N/m^2. Figure 1, taken from [11], uses dynes/cm^2 which is equal to 0.1 Pa. It also plots the wall-shear compliance which is defined as $J^* = 1/G^*$; the larger the value of J^* the more flexible (compliant) the wall will be.

Another simple measure of the viscoelastic damping of a compliant wall can be obtained by dropping a small metal ball from a fixed initial height h_0 and measuring the rebound height h_1; h_1/h_0 is a measure of the energy lost due to viscoelastic damping. In the case of the rotating disk the wall deflections are mainly generated by the pressure and shear–stress perturbations acting on the wall. These can be expected to vary as the square of the linear speed $(\Omega r)^2$ (where Ω is the rotational speed and r is the local radial coordinate). Thus, for a fixed value of elastic modulus, the greater the linear speed the greater the wall deflection. This implies that the effective dimensionless compliance (i.e., deflection produced by unit pressure made

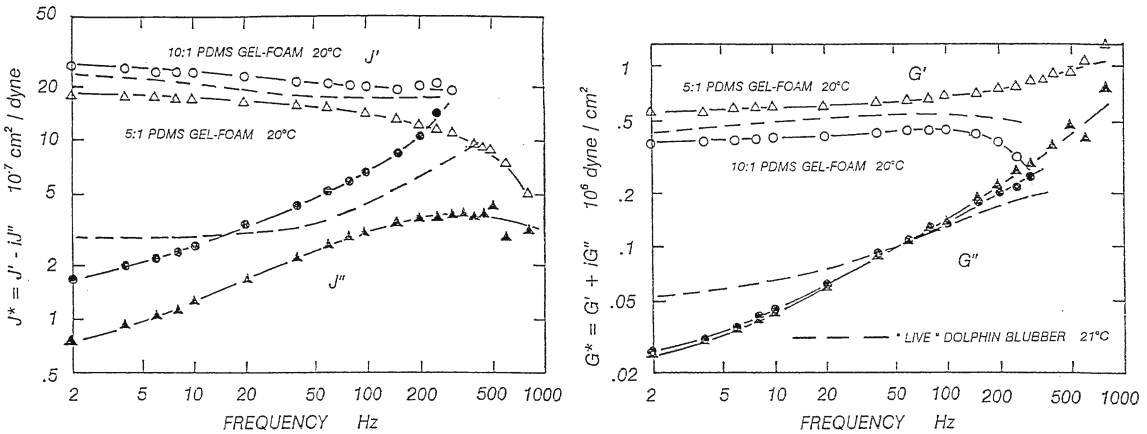

Fig. 1 Frequency variation of shear compliance and modulus J^*, G^*, for 'live' dolphin blubber (dashed lines) compared with those for 10:1 (circles) and 5:1 (triangles) polymer:curing agent polydimethyl siloxane (PDMS) gel-foam composites. (Based on [11, Fig. 2])

non-dimensional with reference to $r/[\rho(\Omega r)^2]$, where ρ is the fluid density) increases as $\Omega^2 r$. So, for a fixed value of elastic modulus, the overall effective compliance varies with Ω^2. It is also evident that in the same case the effective compliance increases with r.

3 Torque measurements on compliant rotating disks

Several investigators have covered disks with compliant material and rotated them in a controlled fashion in a volume of water. This type of arrangement allows one to make the most straightforward drag measurement for a compliant surface by means of accurately measuring the torque required to drive the disk over a range of rotational speeds. A series of experiments of this kind was carried out by Hansen and Hunston [12–14] (a good overview is available in [15]). They used polyvinyl chloride (plastisol) with a wide range of elastic moduli as the material to make single-layer, viscoelastic, compliant walls. This material tends to have a high level of viscoelastic damping. They did not observe any torque reduction, indicative of drag reduction, for any of their compliant disks. In fact, in many cases there was a drag increase. This was probably attributable to the formation of divergence-type instability waves. The critical flow speed for the onset of these waves appeared to be consistent with what was known for flat-plate-type boundary layers over compliant walls (see [7,16]). It is probably fair to say that the main contribution of the work of Hansen and Hunston was the light it shed on the hydroelastic instabilities.

In a later experimental study Chung [17] designed his composite compliant walls with some care and according to certain basic principles suggested by earlier investigators, namely, that the response of the compliant wall should be such as to produce small-amplitude, short-wavelength, high-frequency displacements. Following these principles his composite compliant walls consisted of three main layers:

(i) An inner layer of velvet fabric, 2.5 mm thick, bonded to the metal supporting plate with the velour facing outward. The idea was to produce an anisotropic compliant wall that was resistant to the sort of divergence instability observed by Hansen and Hunston. The fibres were susceptible to buckling but could not be stretched appreciably.
(ii) A layer of silicone rubber, 0.75 mm thick, was cast over the velvet into which it presumably penetrated to act as the matrix material. Lightly cross-linked silicone networks were used in combination with high-viscosity oil.
(iii) Finally a thin, stiff, polymer film was used as an outer covering.

The best results were obtained with a 125 μm thick ptfe (teflon) film.

The concept of the inner anisotropic layer remained unproven, but the thin outer film was found to play an essential role in obtaining a drag reduction. This agrees with the practical findings of Gaster [18] and his co-workers, and the theoretical conclusions of Dixon et al. [19]. Chung also found that high levels of damping were necessary to obtain a drag reduction. For his best compliant walls he obtained the equivalent of 20% drag reduction for a compliant disk rotating in water at an equivalent Reynolds number of 8.92×10^5.

More recently Fitzgerald et al. [11,20–23] in a series of papers have described a research investigation on the material properties of whale and dolphin blubber with a view to mimicking these with artificial compliant walls. They have proposed a model based on electric-circuit theory to describe the fundamental aspects of the interaction between the turbulent boundary layer and a compliant wall. They regard the boundary layer as a 'generator' of fluctuating shear stress that is coupled through the viscous near-wall layer to the 'load' in the form of the compliant wall. In order for appreciable energy, or power, to be transmitted, the shear impedances of the boundary layer (generator) and compliant wall (load) must be matched. And this is thought to be an essential condition for the wall to act to delay laminar–turbulent transition. They use the complex shear compliance, $J^* = J' - \mathrm{j}J''$, as the material property to characterize the wall shear impedance. Recall from Sect. 2 that J^* is linked with the complex shear modulus, G^*, by $G^* = 1/J*$. The shear wave speed is proportional to $\sqrt{G'}$. (Incidentally, the measurements reported in [20] indicate that the shear wave speed for pilot-whale blubber is about 9 m/s.)

Figure 1, from [11], presents the variation of the modulus of shear compliance, $J = \sqrt{J'^2 + J''^2}$, with frequency for 'live' dolphin blubber compared with two artificial compliant materials. (The shear compliance for 'live' dolphin blubber is obtained by measuring it at various times after death and extrapolating back to the time of death.) It can be seen that the gel-foam composites display characteristics that are fairly close to dolphin blubber.

For the experiments of Fitzgerald et al. [11] an aluminium disk with a radius of 10 cm was coated with the PMS compliant materials in order to test their drag-reducing capabilities. Coating thicknesses ranging from 5 to 20 mm were used. The disks were then rotated in a volume of water at speeds ranging from 60 to 2250 RPM. Typical results for torque versus rotational speed are displayed in Fig. 2. There the results for the coated disk are compared with a rigid disk. It can be seen that in both cases an abrupt change of slope occurs at a particular rotational speed. This abrupt change is assumed to be due to laminar–turbulent transition occurring just inboard of the outer radius of the disk. According to this interpretation laminar–turbulent transition occurs at 210 RPM for the rigid disk and at 260 RPM for the compliant disk. Assuming $r = 100$ mm, this is equivalent to raising the transitional Reynolds number $(\Omega r^2/\nu)$ (ν: kinematic viscosity) from approximately 2.2×10^5 to 2.72×10^5. So, use of the compliant disk led to a 24 percent rise in transitional Reynolds number.

4 Flow stability theory for compliant rotating-disk flows

In this section we shall review the recent theoretical research on the effects of wall compliance on the instabilities of the rotating-disk boundary layer. This three-dimensional flow develops over a rotating disk in an initially still ambient fluid. The undisturbed flow field $(\bar{u}, \bar{v}, \bar{w})$ (where these are the velocity components corresponding to the radial r, azimuthal θ, and axial z co-ordinates, respectively) can be modelled by an exact similarity solution of the Navier-Stokes equations first obtained by von Kármán [24] and given by

$$\bar{u} = r\Omega F(z), \qquad \bar{v} = r\Omega G(z), \qquad \bar{w} = \sqrt{\nu\Omega} H(z) \tag{1}$$

where Ω is the rotational speed of the disk and ν is the kinematic viscosity of the fluid. The velocity-profile functions are plotted in Fig. 3.

This relatively simple idealised flow exhibits many of the features found in boundary layers in practical applications. Of particular significance is the cross-flow-vortex instability that results from the inflexion

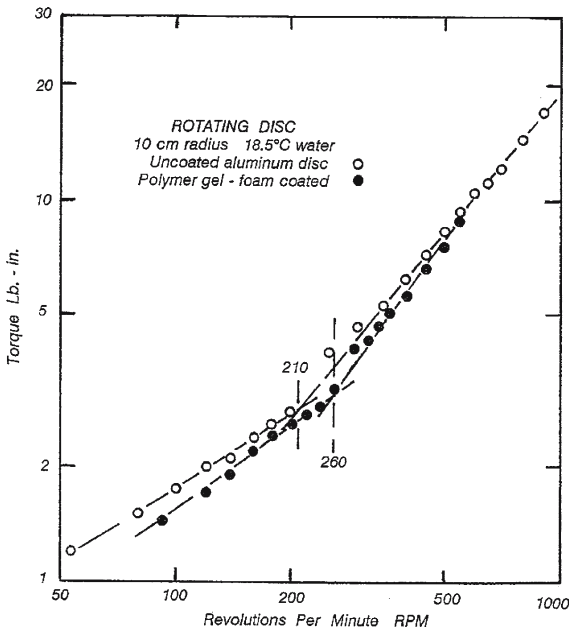

Fig. 2 Drag torque vs. rotational speed for a rigid reference disk (open circles) and for a disk coated with a 4.85 mm thick polymethyl siloxane gel-polyurethane foam and a smooth, 0.15 mm thick, outer layer of natural rubber latex (filled circles). (Based on [11, Fig. 6])

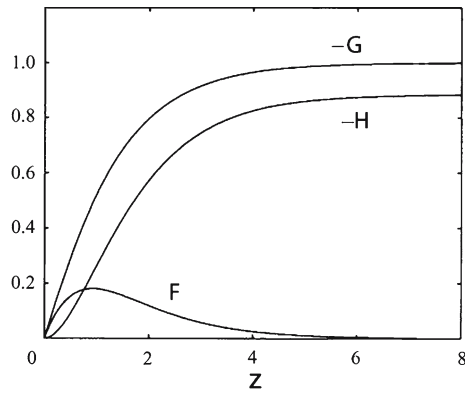

Fig. 3 The Kármán [24] solution for the radial *(F)*, azimuthal *(G)*, and axial *(H)* velocity components for boundary-flow flow over a rotating disk

point in the radial component of the velocity profile. It is this form of instability that can lead to transition for flows over swept leading edges. Although the primary instability mechanism for the cross-flow vortices is essentially inviscid, viscous effects must be considered in the stability analysis if growth rates are to be represented accurately. Including viscous terms in the usual sense results in the well-known Orr–Sommerfeld equation. In the case of the rotating disk, however, this fourth-order equation is not sufficient for a good representation of the instability characteristics because it omits effects like Coriolis acceleration. Lilly [25] first established that the inclusion of Coriolis acceleration terms significantly affected the stability characteristics of the related Ekman boundary layer. Later Malik et al. [26] demonstrated that Coriolis and streamline-curvature effects have a significant stabilizing effect on the disturbances developing in the rotating-disk boundary layer. Including both of these effects results in a sixth-order system of ordinary differential equations that reduces to the Orr–Sommerfeld equation when the Coriolis and streamline curvature terms are omitted. Cooper and Carpenter [27] showed how this system of instability equations may be coupled to the Navier equations of motion for a viscoelastic solid in order to model the dynamics of a boundary-layer disturbance developing interactively over a single viscoelastic layer.

The instability of the boundary layer over a rigid rotating disk has been studied extensively and the characteristic features of the eigenmode spectrum are quite complex; at least three distinct families of eigensolutions have been identified. One is the inviscid or Type I instability (i.e., the cross-flow vortices mentioned above) first studied by Gregory et al. [8] who were followed by notable contributions from Malik et al. [26], Wilkinson and Malik [28] and Mack [29]. This form of instability is considered to be the commonest route to transition and has been well studied experimentally. The early work by Gregory et al. using a china-clay visualisation technique was able to reveal the cross-flow instability clearly as a series of closely spaced spiral streaks that are stationary relative to the disk surface. Mack successfully modelled theoretically the modulated disturbance forms observed experimentally by Wilkinson and Malik, thereby

establishing that they result from a superposition of the complete, zero-frequency, azimuthal wavenumber spectrum. He also noted that, although the experimentally observed spiral streaks correspond to zero-frequency disturbances, they are not the most unstable modes in the boundary layer. Some travelling modes were found to have a higher growth rate than the stationary ones. More comprehensive information on the theoretical stability characteristics of travelling modes was supplied by Balakumar and Malik [30] who confirmed Mack's results.

Until fairly recently the role of the travelling disturbances in experiments on transition remained fairly obscure. This was despite the fact that in the first experimental study of instability of the rotating- disk boundary layer Smith [31] used two hot-wire probes and detected travelling disturbances. Recently, however, travelling modes have been detected and studied experimentally. Jarre et al. [32,33] (see also [34] and [35]) have carried out 2-point measurements with hot-film probes enabling them to measure phase speeds. Jarre et al. [32] found that, for the natural transition process over a nominally smooth disk, travelling waves dominated in the early stages of instability. For the later stages, when the disturbances had reached a larger amplitude, stationary disturbances (i.e., zero-frequency modes) dominated. Jarre et al. [33] then studied the case when transition is forced with a roughness element placed at a position just inboard of the location corresponding to the linear threshold for Type I instability. The roughness element was of a size comparable to the boundary-layer thickness and accordingly generated finite-amplitude disturbances. Nevertheless one might have expected strong stationary disturbances to have dominated the transition process. What was found instead was that the dominant disturbances had a small, but definite, negative phase speed, i.e., they travelled with a circumferential phase speed slightly less than the disk rotation speed. The range of propagation angles at this phase speed agreed well with the theoretical predictions of Balakumar and Malik [30]. But, owing to finite-amplitude effects, good agreement with linear stability theory was not found in other respects. It is probably true, however, that the most dramatic role played by the travelling modes is to generate absolute instability. This was discovered by Lingwood [36,37] and will be discussed below.

A second family of eigenmodes, termed Type II, contains a weaker, viscous instability that appears only when Coriolis effects are included. A similar instability was first discovered in the Ekman boundary-layer by Faller [38]. In the rotating-disk boundary layer the stationary form of this instability typically appears at higher Reynolds numbers than the Type I mode and Coriolis acceleration is essential for its occurrence, but little else is known about the precise physical instability mechanism or the role of this mode in the transition process. However, clear evidence of the existence of Type II instabilities has been revealed by Lingwood [37] in her experimental study of the impulsively perturbed rotating-disk flow. Lingwood [36] also noted that the Types I and II coalesce at a point just inboard of the critical Reynolds number (defined as $R = r\sqrt{\Omega/\nu}$) where both eigenmodes are convectively stable. In this case algebraic growth results (as first suggested in the context of the Orr–Sommerfeld equation by Koch [39]) rather than absolute instability. This could have been physically significant and has recently been confirmed in numerical simulations reported by Davies and Carpenter [40]. But for the rigid disk, at least, their simulations show that the algebraic growth is dominated by the exponentially growing Type I instability that sets in at a slightly more outboard radial position.

A third family of eigenmodes, which we will term Type III, was first identified by Mack [29] and briefly mentioned by Balakumar and Malik [30]. These eigenmodes are found to have large negative values of α_i (where $\alpha = \alpha_r + \mathrm{i}\alpha_i$ is the radial wavenumber) but are considered to be strongly stable modes in view of their inwardly directed group velocity. Lingwood [36] has shown that this Type III can coalesce with the Type I instability to form an absolute instability, thereby providing another route to transition. This seemed to be confirmed experimentally in [37], but see comments below.

The effects of wall compliance on the Types I and II instability have been studied theoretically by Cooper and Carpenter [27]. The form of compliant wall used in their study was a single layer of viscoelastic material. Since any disturbances created by the interaction of the boundary layer and the compliant wall tend to attenuate rapidly as they propagate into the wall, Cooper and Carpenter carried out their

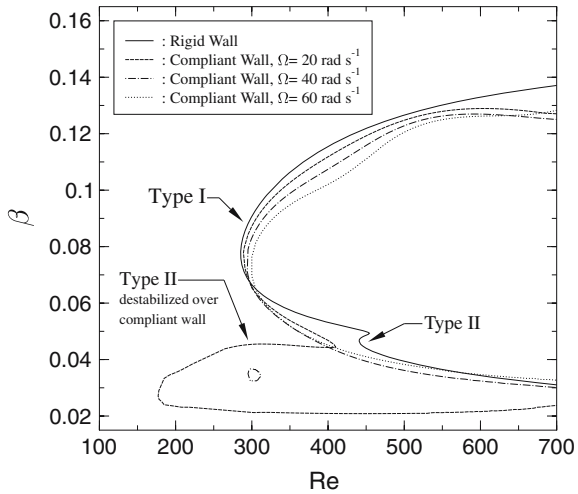

Fig. 4 Neutral curves for stationary disturbances over rigid and compliant rotating disks showing the variation of the azimuthal wave-number β with Reynolds number R according to the theory of Cooper and Carpenter [27]. Solid grey curve rigid wall; compliant wall: - -, $\Omega = 20$ rad/s; —, $\Omega = 40$ rad/s; · · ·, 60 rad/s. (Based on [27, Fig. 2a])

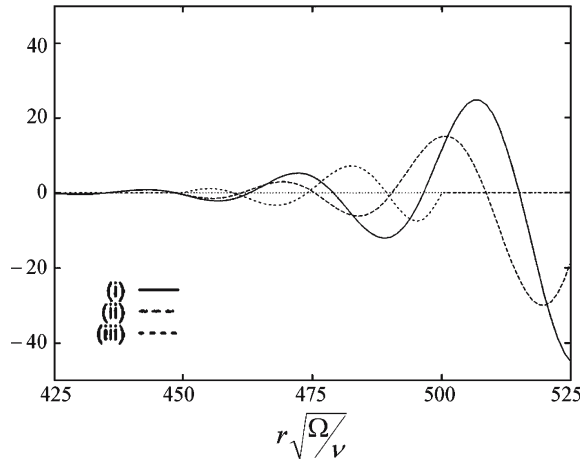

Fig. 5 Instantaneous dimensionless surface displacements and pressure perturbations at the disk surface obtained by numerical simulation for a Type I disturbance with azimuthal wave-number $n = 43$ excited impulsively at $r\sqrt{\Omega/\nu} = 400$. (i) Pressure for an entirely rigid disk, (ii) pressure at the same instant of time in the periodic forcing cycle when there is a compliant annulus extending from $r\sqrt{\Omega/\nu} = 450$ to $r\sqrt{\Omega/\nu} = 500$, (iii) corresponding dimensionless compliant-surface displacements. The compliant wall parameters are such that, notionally, there is marginal stability with respect to divergence and travelling-wave flutter at the outermost radius of the annulus. (Based on [40, Fig. 8])

instability calculations for an infinitely deep compliant layer. They chose a modulus of rigidity, $G = 1000$ N/m^2 and varied the effective compliance of the disk by varying the rotational speed. Typical results for neutral-stability curves of the stationary eigenmodes are displayed in Fig. 4. It is found that, as the rotational speed (effective wall compliance) is increased, there is an increasing stabilizing effect on the Type I instability. This is confirmed by the results for the growth rate given in [27] and the results of the numerical simulations by Davies and Carpenter [40] plotted in Fig. 5. This depicts the stabilizing effect on the Type I instability of an annular region of compliant wall inset into an otherwise rigid disk. The compliant wall extends from $r\sqrt{\Omega/\nu} = 450$ to $r\sqrt{\Omega/\nu} = 500$. In this case the wall dynamics are modelled theoretically by the plate–spring compliant wall [41]. The wall properties are chosen so that there is marginal stability with respect to the hydroelastic instabilities at the outer radius of the annulus.

It is clear from Fig. 4 that the effect of wall compliance on the Type II instability is more complex. For the rigid wall the critical Reynolds number for the stationary Type II instability is about 440. For relatively low levels of wall compliance (low rotational speed) the effect is strongly destabilizing. Note that for $\Omega = 20$ rad/s the enlarged area of instability is quite striking and the critical Reynolds number falls to 177. However, as the degree of effective wall compliance is raised further this unstable region shrinks and ultimately vanishes for $\Omega = 60$ rad/s.

Since the Type II instability is destabilized for moderately compliant walls, it is only to be expected that wall compliance will also promote the appearance of modal coalescence between the Types I and II eigenmodes. Cooper and Carpenter [27] showed that for rigid walls modal coalescence first occurs at $R = 437$ (where both eigenmodes are stable), just a little ahead of the value of $R = 439$ where its occurrence coincides with neutral stability of the Type I instability. But for a disk with a relatively low level of compliance (i.e., a rotation speed of 20 rad/s) the corresponding two Reynolds numbers are $R = 373$ and

387. So it is possible that the algebraic growth associated with the modal coalescence is physically more significant for a compliant disk. But this has not been confirmed.

A more important phenomenon is the absolute instability discovered by Lingwood [36,37] for which the critical Reynolds number is 507 (this corrected value is given in [42]). This comes about through a coalescence of the Type I and Type III eigenmodes. Cooper and Carpenter [43] showed theoretically that even a small degree of wall compliance is enough to substantially postpone the absolute instability or even suppress it completely. However, recently Davies and Carpenter [44] have presented a study based on numerical simulations, essentially computational experiments, using the full linearized Navier–Stokes equations with the inhomogeneous spatial variation, the so-called non-parallel terms, included—these terms were omitted in the stability analyses of Lingwood and of Cooper and Carpenter. This has led to a re-interpretation of Lingwood's theory and experimental investigation. Essentially, Davies and Carpenter [44] have shown that the absolute instability does not lead to a global-instability mode and that convective instability dominates throughout. Nevertheless, their simulations reproduce the features seen in the experiments of Lingwood [37].

The analysis of finite-amplitude crossflow vortices in the rotating-disk boundary layer carried out by Pier [45] confirmed that no linear global mode was associated with the absolute instability. Instead Pier found that transition occurred due to secondary absolute instability of the naturally selected primary nonlinear crossflow vortices. Very recently, a careful, high-quality, experimental investigation has been carried out by Othman and Corke (see [46] and [47]). Among other things this investigation confirms the main findings of Davies and Carpenter [44] and reports a transitional Reynolds number well in excess of the critical Reynolds number for absolute instability. This does not imply that there was any fault in Lingwood's original analysis. Rather it is a question of how to interpret both her theory and experiment.

In the numerical simulations of Davies and Carpenter [44] the existence of absolute instability is associated with transient temporal growth, rather than unlimited temporal growth as expected for an absolute instability and found in Lingwood's theory or numerical simulations based on the artificial homogeneous flow field. Davies and Carpenter also performed some numerical simulations with part of the disk's surface replaced by an annulus of compliant material. The absolute instability, in accordance with the findings of Cooper and Carpenter [43], is eliminated over the compliant annulus. The presence of the compliant wall greatly weakens the transient temporal growth. Moreover, the compliant wall exerts a strong stabilizing influence on the flow over the rigid disk *upstream* of its leading edge. In fact, as time progresses, the inboard upstream influence of the compliant wall becomes more extensive.

Finally, we shall briefly refer to two studies on the effects of wall compliance on stability in other rotating systems. Namely, the study by Koga and Nagata (described in [48]) of the effects of wall compliance on the stability of Taylor-Couette flow. And also, the study of Allen and Bridges [49] on the hydrodynamic stability of the Ekman boundary layer over a compliant wall.

5 Experimental studies of disturbance evolution in compliant rotating-disk flows

The first experiments on the evolution of boundary-layer disturbances over a compliant rotating disk were carried out by Colley et al. [50]. Their compliant walls were manufactured from a single layer of silicone rubber having a typical elastic modulus of 400 kPa which corresponded to a comparatively low effective compliance at the rotational speed of 7.85 rad/s used in their experiments. They followed fairly closely the methodology of Jarre et al. [32–34] in terms of both the overall set-up and the use of a series of Fourier spectra (e.g., see Fig. 7) to determine the growth rates and other characteristics of the disturbances. Thus, the disk rotated within an inner partial enclosure with the whole contained in a larger tank filled with water. The enclosure consisted of a lid with an annular side wall. The height of the lid above the surface was large compared with the boundary-layer displacement thickness.

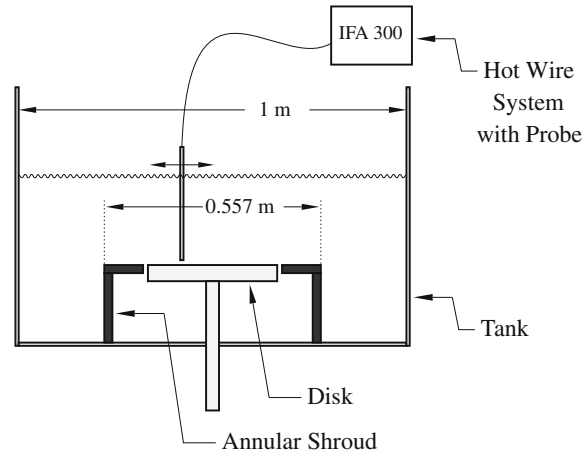

Fig. 6 The new rotating-disk apparatus used by Colley et al. [52]

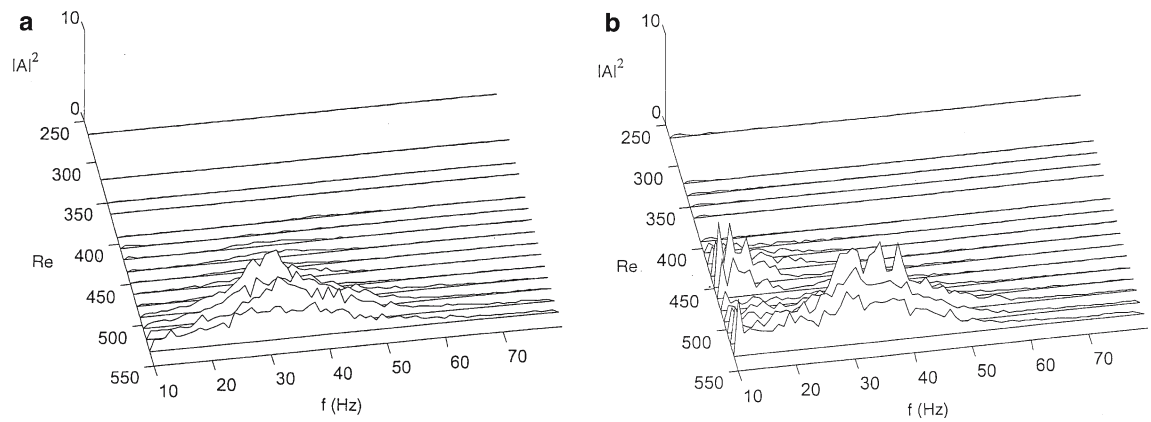

Fig. 7 Spectra at various values of Reynolds number obtained by Colley et al. [52] for (**a**) a rigid disk, and (**b**) a compliant disk, both rotating at 1.25 rev/s

Colley et al. showed that the compliant disk had a stabilizing effect on the Type I, cross-flow vortex, eigenmode. Nevertheless, transition actually occurred earlier than for the rigid disk, although the turbulence level during and after transition was significantly lower for the compliant disk. These observations appear to be consistent with the theoretical study of Cooper and Carpenter [27] which showed that wall compliance had a stabilizing effect on the Type I instability and that low to moderate levels of wall compliance destabilized the viscous Type II mode. It could therefore be argued that it was the latter that provided the route to transition. In an important respect, however, the experimental results were not consistent with the theory. This is because the theory suggests that the effects of compliant walls as stiff as those used in the experiments should produce results that are indistinguishable from those found for a rigid disk.

In their more recent experimental study Colley et al. [51,52] redesigned their rotating-disk apparatus as shown in Fig. 6. The new set-up has dispensed with the cover over the rotating disk used in Colley et al. [50] and instead added an annular shroud. This shroud is designed to prevent the disturbed flow created in the region on the underside of the disk from disturbing the flow over the test surface. The new configuration appears to be much superior to the old one in terms of background noise and it is much easier to make measurements. The undisturbed velocity profiles are virtually identical to those reported in [50, Fig. 2].

The new apparatus was used to study the development of boundary-layer disturbances over a softer compliant disk. This was manufactured from MED 6340 silicone rubber that had a typical modulus of elasticity, $E = 80\,\text{kPa}$. Successive Fourier spectra for a range of radial positions corresponding to the rigid and

Table 1 Transitional Reynolds numbers for the rigid and ($E = 80\,\text{kPa}$) compliant disks

Ω rad s^{-1}	Re_t (rigid)	Re_t (compliant)
1.25π	c. 510	c. 520
2.5π	c. 510	c. 520
3.0π	c. 520	c. 540

compliant disks are presented in Fig. 7. It can be seen that, for the rigid disk, only the Type I disturbance, corresponding to the central peaks of the spectra, is present. Note that the final spectrum is broadband which is indicative of fully turbulent flow. For the compliant disk there is a Type II disturbance also present exemplified by the spectral peaks seen at lower frequencies and lower Reynolds number. (Note that the probe is stationary so that the disk with its stationary vortex-like disturbances rotates below it. Thus, temporal frequency is really a measure of azimuthal wave-number.) Accordingly, it can be seen that in terms of the the value of the azimuthal wave-number, the results in Fig. 7 are quantitatively in good agreement with the theory of Cooper and Carpenter [27] as illustrated in Fig. 4. Furthermore, qualitatively at least, the experimental results support the surprising discovery of the theory that low to moderate levels of wall compliance greatly advance the critical Reynolds number for the Type II disturbance. This is evident from a comparison between Fig. 7a and b.

Unlike the early investigation of Colley et al. [50], modest transition delays were found by Colley et al. [52]. These are summarized in Table 1.

6 Experimental studies of thin-gap rotating flows

The flow in a fluid-filled gap between a rotating disk (rotor) and a stationary enclosure (stator) is of practical and fundamental interest [53]. The fluid motion is driven by the rotor but boundary layers are established on both, the rotor and the stator. The laminar–turbulent transition process of the flow is governed by the Reynolds number $\text{Re} = \Omega r^2/\nu$ and the ratio, $\bar{h} = h/r_\text{d}$ of gap width, h, and disk radius, r_d.

Flow visualization experiments by Schouveiler et al. [10,54,55] have revealed two different transition scenarios for gap widths larger or smaller than the combined thickness of the two boundary layers on rotor and stator. When the gap is wider than this combined thickness, circular and spiral waves are observed to destabilize the stationary-disk boundary layer. Transition occurs in this case by mixing of these waves. When the gap is narrower, such that the rotor and stator boundary layers merge, finite-size turbulent structures can appear. These structures consist of turbulent spots or turbulent spirals which penetrate the laminar domains of the flow as the Reynolds number is increased [55].

Recently research groups at the University of Warwick and I.R.P.H.E, Marseille initiated a collaborative experimental investigation studying transition over the type of compliant disks used by Colley et al. [50–52] employing the narrow-gap rotating-disk facility of Schouveiler et al. [10,54,55]. The parameter range covered in their initial experiments was $\text{Re} \leq 4.2 \times 10^5$ with $0.005 \geq \bar{h} \geq 0.02$.

Compliant disks were manufactured from Silicon Gel (NuSil MED-6340, Polymer Systems Technology Ltd., High Wycombe, UK). The gel is supplied in two separate components. Varying the mixing ratio of the components enables producing compliant surfaces with different elastic moduli. Two disks were manufactured at Warwick and tested at Marseille.

The first disk was fabricated using a 1:1 mixing ratio of the gel components. The elastic modulus and the damping coefficient were determined by the techniques described in [50]. The elastic modulus was $E = 326\,\text{kPa}$ and the damping coefficient corresponded to $\log(h_0/h_1) = 1.33 \pm 0.05$, (where h_0 and h_1 are the initial and rebound heights of a small metal ball). The experiments revealed that this compliance level did not measurably affect the critical Reynolds numbers for the onset and the disappearance of the wave structures observed by Schouveiler et al. [10,54,55] for rigid disks.

The second disk was more compliant. It was fabricated from a 2:1 gel mixture (2 parts component A and 1 part component B). The elastic modulus was 267 kPa while its damping coefficient was $\log(h_0/h_1) = 3.11 \pm 0.05$. This level of compliance was found to affect the transition process [9]. It was, for instance, observed that the onset for the occurrence of the spiral waves was postponed to higher disk speeds. The delay depends on $\bar{h}$ and lies, typically, between 10% (for onset) 60% (for disappearance) above the values measured for the rigid disk. The solitary waves evolve directly from defects of the primary spiral waves and, hence, onset delays of similar magnitude were observed for these structures. The threshold velocity for the emergence of turbulent spots over the compliant disk remained unchanged, however, with regard to the values measured by Schouveiler et al. [10,54,55] for rigid disks. A detailed discussion of these results is given in [9].

7 Conclusion

First, we reviewed the experimental studies whereby the driving torque for the rotating disk is determined as a measure of drag. This type of test has its drawbacks: principally the lack of direct information about the fluid and solid mechanics. They are also more difficult to do well than their simple conceptual basis would suggest. Nevertheless, there have been worthwhile studies of this kind that reveal sharp changes in slope of the relationship between torque and rotational speed. This feature is indicative of laminar–turbulent transition. In this way Fitzgerald et al. [11,22] demonstrated a delay in transition, reflected through a 24 percent rise in transitional Reynolds number, with their compliant (analogue dolphin blubber) disks.

We then reviewed the studies of boundary-layer instability over compliant rotating disks. The main outcomes of these studies are that: (i) wall compliance tends to stabilize the Type I cross-flow-vortex eigenmode; (ii) very moderate levels of compliance suppress the absolute instability; and (iii) the effect of wall compliance on the viscous Type II eigenmode is complex; low-to-moderate levels of compliance greatly reduce the critical Reynolds number, whereas higher levels of compliance stabilize and even completely eliminate the instability. The experimental studies reviewed confirm the stabilizing effect on the Type I instability. As regards the absolute instability, according to the recent numerical-simulation study of Davies and Carpenter [44] and experimental investigation of Othman and Corke [47], the absolute instability is not associated with a global mode and convective behaviour dominates throughout. Nevertheless, wall compliance still has a very marked stabilizing effect on the disturbances due to the absolute instability found in the real inhomogeneous flow. Finally, the very recent experimental study of Colley et al. [52] fully confirms the destabilizing effects of wall compliance on the Type II instability. This last result demonstrates that a theoretical model combining linearized equations of motion for the flow field and solid mechanics is capable of predicting the behaviour of instabilities in the real flow. The experimental studies of Colley and Carpenter [51] and Colley et al. [52] also reveal a small rise in the transitional Reynolds number.

The favourable effects of wall compliance on laminar–turbulent transition for rotating-disk boundary layers are somewhat disappointing in comparison with laminar-flow capabilities of compliant walls for quasi-two-dimensional boundary layers. One reason, perhaps, is that the theory and the more detailed experimental studies have focused on single-layer homogeneous compliant walls. It is well known that this type of compliant wall has a much reduced laminar-flow capability compared with two-layer walls (see, for example, [19]). In addition to this, the destabilizing effect of wall compliance on the Type II instability tends to advance transition. All this suggests that it would be worthwhile to investigate the effects of compliant disks with more complex two- or multi-layer structures on boundary stability and laminar–turbulent transition.

Lastly, given the established laminar-flow capability of appropriately designed compliant walls, one might ask about actual and potential industrial applications. A major disadvantage of compliant walls is that they are not really a viable technology for aeronautical applications [5]. In principle, one could design a compliant wall for laminar-flow control in air. The problem is that, owing to the need to match the

inertias of the fluid and solid media, impractically flimsy compliant walls would be required for operation in air. It has been firmly established that compliant walls are a viable technology for marine applications. The practical problem in this case is that a fairly substantial investment in developing suitable durable materials and novel manufacturing techniques would be required to turn it into a practical drag-reduction technology. With the end of the Cold War, the desire for drag reduction on submarines and other naval vessels has diminished. On the other hand, the civil marine industry is rather fragmented and lacks a coherent investment plan in drag reduction. The various competing teams in the Americas Cup competition represent one sector of marine activity willing to invest in novel drag-reduction technology. Unfortunately, the use of compliant walls is expressly forbidden under the Americas Cup rules. Probably, the most promising industrial application for compliant walls is to be found in water and oil pipelines. In both cases it has for some time been the practice to use substantial amounts of polymer additives to reduce drag and thereby pumping requirements. One could expect suitably designed compliant walls could eliminate or substantially reduce the need for such additives.

References

1. Gray J (1936) Studies in animal locomotion, VI. The propulsion powers of the dolphin. J Exp Biol 13:192–199
2. Carpenter PW, Davies C, Lucey AD (2000) Hydrodynamics and compliant walls: Does the dolphin have a secret? Current Sci 79:758–765
3. Riley JJ, Gad-El-Hak M, Metcalfe M (1988) Compliant coatings. Ann Rev Fluid Mech 20:393–420
4. Carpenter PW (1997) Status of transition delay using compliant walls. Prog Astronaut Aeronaut 123:79–113
5. Carpenter PW, Lucey AD, Davies C (2001) Progress on the use of compliant walls for laminar-flow control. J Aircraft 38:504–512
6. Gad-El-Hak M (1996) Compliant coatings: a decade of progress. Appl Mech Rev 49:S1–S11
7. Gad-El-Hak M (2003) Drag reduction using compliant walls. In: Carpenter PW, Pedley TJ (eds) Flow past highly Compliant Boundaries and in collapsible tubes. Fluid Mechanics and its Applications, Kluwer Academic Publishers, vol 72. pp 191–229
8. Gregory N, Stuart JT, Walker WS (1955) On the stability of three-dimensional boundary layers with application to the flow due to a rotating disk. Phil Trans R Soc London Ser A 248:155–199
9. Cros A, Ali R, Le Gal P, Thomas PJ, Schouveiler L, Carpenter PW, Chauve MP (2003) Effects of wall compliance on the laminar–turbulent transition of torsional Couette flow. J Fluid Mech 481:177–186
10. Schouveiler L, Le Gal P, Chauve MP (1999) Spiral and circular waves in the flow between a rotating and a stationary disk. Exp Fluids 26:179–187
11. Fitzgerald ER, Fitzgerald JW (1998) Blubber and compliant coatings for drag reduction in water. V. Driving point shear impedance measurements on compliant surfaces. In: Meng JCS (ed) Proc Int Symp on Seawater Drag Reduction, 22–23 July, Newport, RI, USA, pp 211–214
12. Hansen RJ, Hunston DL (1974) An experimental study of turbulent flows over compliant surfaces. J Sound Vib 34(3):297–308
13. Hansen RJ, Hunston DL (1976) Further observations on flow-generated surface waves in compliant surfaces. J Sound Vib 46:593–595
14. Hansen RJ, Hunston DL (1983) Fluid-property effects on flow-generated waves on a flexible surface. J Fluid Mech 133:161–177
15. Hansen RJ, Hunston DL, NI CC, Reischman MM, Hoyt JW (1980) Hydrodynamic drag and surface deformations generated by liquid flows over flexible surfaces. Prog in Astronaut Aeronautics, 72:439–452
16. Gad-El-Hak M, Blackwelder RF, Riley JJ (1984) On the interaction of compliant coatings with boundary layer flows. J Fluid Mech 140:257–280
17. Chung KH (1985) Composite compliant coatings for drag reduction utilising low modulus high damping silicone rubber. Ph. D. Thesis, MIT
18. Gaster M (1987) Is the dolphin a red herring? In: Liepmann HW, Narasimha R (eds) Proc IUTAM Symp on Turbulence Management and Relaminarisation. Springer, Bangalore India, pp 285–304
19. Dixon AE, Lucey AD, Carpenter PW (1994) Optimization of viscoelastic compliant walls for transition delay. AIAA J 32:256–267
20. Fitzgerald ER, Fitzgerald JW (1995) Blubber and compliant coatings for drag reduction in water. I. Viscoelastic properties of blubber and compliant coating materials. Mat Sci Eng C 2:209–214
21. Fitzgerald JW, Fitzgerald ER, Carey WM, von Winkle WA (1995) Blubber and compliant coatings for drag reduction in water. II. Matched shear impedance for compliant layer drag reduction. Mat Sci and Engng C 2:215–220

22. Fitzgerald JW, Fitzgerald ER, Martin JE (1998) Blubber and compliant coatings for drag reduction in water. III. Rotating disc drag measurements that mimic dolphin blubber. In: Tomlinson GR, Bullough WA (eds) Smart Materials and Structures. IOP Pub. Ltd., Bristol, UK, pp 543–550
23. Fitzgerald JW, Martin JE, Modert EF (1998) Blubber and compliant coatings for drag reduction in water. VI. Rotating disc apparatus for drag measurement on compliant layers. In: Meng JCS (ed) Proc Int Symp on Seawater Drag Reduction, 22–23 July, Newport, RI, USA, pp 215-218
24. von Kármán Th (1921) Über laminare und turbulente Reibung. Zeitschrift für angewandte Mathematik und Mechanik 1:233–252
25. Lilly DK (1966) On the instability of Ekman boundary flow. J Atmos Sci 23:481–494
26. Malik MR, Wilkinson SP, Orszag SA (1981) Instability and transition in rotating disk flow. AIAA J 19:1131–1138
27. Cooper AJ, Carpenter PW (1997) The stability of rotating-disc boundary-layer flow over a compliant wall. Part 1. Type I and II instabilities. J Fluid Mech 350:231–259
28. Wilkinson SP, Malik MR (1985) Stability experiments in the flow over a rotating disk. AIAA J 23:588–595
29. Mack LM The wave pattern produced by point source on a rotating disk. AIAA Paper 85-0490.
30. Balakumar P, Malik MR (1990) Travelling disturbances in rotating-disk flow. Theor and Comp Fluid Dyn 2:125–137
31. Smith NH (1946) Exploratory investigation of laminar-boundary-layer oscillations on a rotating disk. N.A.C.A. TN 1227
32. Jarre S, Le Gal P, Chauve MP (1996) Experimental study of rotating disk instability. I. Natural flow. Phys Fluids 8:496–508
33. Jarre S, Le Gal P, Chauve MP (1996) Experimental study of rotating disk instability. II. Forced flow. Phys Fluids 8:2985–2994
34. Jarre S, Le Gal P, Chauve MP (1991) Experimental analysis of the instability of the boundary layer over a rotating disk. Europhys Lett 14:649–654
35. Le Gal P (1992) Complex demodulation applied to the transition to turbulence of the flow over a rotating disk. Phys Fluids A 4:2523–2528
36. Lingwood RJ (1995) Absolute instability of the boundary layer on a rotating disk. J Fluid Mech 299:17–33
37. Lingwood RJ (1996) An experimental-study of absolute instability of the rotating-disk boundary-layer flow. J Fluid Mech 314:373–405
38. Faller AJ (1963) An experimental study of the instability of the laminar Ekman boundary layer. J Fluid Mech 15:560–576
39. Koch W (1986) Direct resonance in Orr-Sommerfeld problems. Acta Mech 58:11–29
40. Davies C, Carpenter PW (2001) A novel velocity-vorticity formulation of the Navier-Stokes equations with applications to boundary-layer disturbance evolution. J Comp Phys 172:119–165
41. Carpenter PW, Garrad AD (1985) The hydrodynamic stability of flows over Kramer-type compliant walls. Pt 1. Tollmien-Schlichting Instabilities. J Fluid Mech 155:456–510
42. Lingwood RJ (1997) Absolute instability of the Ekman layer and related rotating flows. J Fluid Mech 331:405–428
43. Cooper AJ, Carpenter PW (1997) The stability of rotating-disc boundary-layer flow over a compliant wall. Part 2. Absolute instability. J Fluid Mech 350:261–270
44. Davies C, Carpenter PW (2003) Global behaviour corresponding to the absolute instability of the rotating-disc boundary layer. J Fluid Mech 486:287–329
45. Pier B (2003) Finite-amplitude crossflow vortices, secondary instability and transition in the rotating-disk boundary layer. J Fluid Mech 487:315–343
46. Othman H (2005) Experimental study of absolute instability of a rotating-disk boundary layer. PhD dissertation, University of Notre Dame, USA
47. Othman H, Corke TC (2006) Experimental investigation of absolute instability of a rotating-disk boundary layer. J Fluid Mech 565:63–94
48. Carpenter PW, Thomas PJ, Nagata M (2003) Rotating flows over compliant walls. In: Carpenter PW, Pedley TJ (ed) Flow past highly Compliant Boundaries and in collapsible tubes. Fluid Mechanics and its Applications, Kluwer Academic Publishers, vol 72. pp 167–187
49. Allen L, Bridges TJ (2003) Hydrodynamic stability of the Ekman boundary layer including interaction with a compliant surface: a numerical framework. Euro J Mech B/Fluids 22:239-258
50. Colley AJ, Thomas PJ, Carpenter PW, Cooper AJ (1999) An experimental study of boundary-layer transition over a rotating, compliant disc. Phys Fluids 11:3340–3352.
51. Colley AJ, Carpenter PW (2000) Experiments on boundary-layer transition over a rotating compliant disc – New experimental method. In abstracts of: 4th EUROMECH Fluid Mech. Conf., Eindhoven, The Netherlands, 19–23 November
52. Colley AJ, Carpenter PW, Thomas PJ, Ali R, Zoueshtiagh F (2006) Experimental verification of Type-II-eigenmode destabilization in the boundary layer over a compliant rotating disk. Phys Fluids 18:054107
53. Owen JM, Rogers RH (1989) Flow and heat transfer in rotating-disc Systems, vol. 1 - Rotor-Stator Systems. Research Studies Press Ltd., Taunton, Somerset, UK
54. Schouveiler L, Le Gal P, Chauve MP (1998) Stability of a travelling roll system in a rotating disk flow. Phys Fluids 10:2695–2697
55. Schouveiler L, Le Gal P, Chauve MP (2001) Instabilities of the flow between a rotating and a stationary disk. J Fluid Mech 443:329–350